Ceiling Jet Flow Properties for Flames Impinging on an Inclined Ceiling

Yasushi OKA[1], MASAKI ANDO[2], and KYOKO KAMIYA[2]
[1]Faculty of Environment and Information Sciences
Yokohama National University
79-7 Tokiwadai, Hodogaya-ku, Yokohama, 240-8501, Japan
[2]Graduate School of Environment and Information Sciences
Yokohama National University
79-7 Tokiwadai, Hodogaya-ku, Yokohama, 240-8501, Japan

ABSTRACT

Many theoretically and/or experimentally derived correlations have been proposed for predicting the temperature rise, velocity, and optical smoke concentration at given radial positions in the ceiling jet that is generated by a steady and time-dependent fires under flat ceilings. Fewer studies have considered the ceiling jet flow generated by a steady fire below an inclined smooth ceiling. The current study addresses the ceiling jet that is generated from a comparatively large fire source, where flames touch a sloped ceiling having an inclination angle of up to 40°. Experiments were conducted to investigate the effect of inclination angle on ceiling jet properties. Temperature and velocity distributions in ceiling jet were measured in detail using a thermocouple rake and a particle imaging velocimetry (PIV) system. Velocity was also measured using bi-directional flow probes. Based on these data, the decrease in temperature rise and velocity along the steepest run in the upward direction, horizontal distribution of temperature in the spanwise direction and the Gaussian momentum and thermal thickness were discussed. Empirical formulae for these parameters are presented.

KEYWORDS: ceiling jet, unconfined inclined ceiling, temperature, velocity, Gaussian momentum, thermal thickness, flame.

NOMENCLATURE LISTING

a, b, c	Coefficients
D	length of fuel pan (m)
e	Napier's constant
H	ceiling clearance (m)
L	length defined by $H/\sin\theta + r_{up}$ (m)
L_T	Gaussian thermal thickness (m)
L_V	Gaussian momentum thickness (m)
r	radial distance from the plume impinged point (m)
V	velocity (m/s)
ΔT	temperature rise (K)
$\Delta T_{\text{spanwise,L}}$	temperature rise away from the plume centreline in the spanwise direction at distance of L (K)
$\Delta T_{\text{up,L}}$	temperature rise at distance of L along the steepest run passing through the ceiling centre (K)
z	distance perpendicular to ceiling surface (m)
z'	distance perpendicular to ceiling surface from the estimated maximum temperature point to ceiling surface, not the distance from the ceiling (m)
Q^*	dimensionless heat release rate $= Q/(\rho_\infty C_p T_\infty g^{1/2} H^{5/2})$

Greek

α, β	coefficient
ε	relative error
γ	spread width approximated by normal distribution (-)
η	dimensionless distance defined by r_{hori}/L (-)
δT	thermal boundary layer thickness (m)
δV	momentum boundary layer thickness (m)

subscripts

down	downward
max	maximum
mean	mean
up	upward
down	downward
span	spanwise
∞	atmosphere

FIRE SAFETY SCIENCE-PROCEEDINGS OF THE TENTH INTERNATIONAL SYMPOSIUM, pp. 471-482
 / DOI: 10.3801/IAFFS.FSS.10-471

INTRODUCTION

Knowledge of ceiling jet velocity and gas temperature is required to design effective installation positions and detection levels for operation of heat detector or fire sprinkler systems. Hence, characterizing the ceiling jet formed by a fire-induced buoyant plume is essential, since most fire detection and suppression devices are designed to operate within the ceiling jet.

Many researchers [1–6] have recorded detailed velocity and temperature measurements of hot currents generated by both steady and time-dependent fires below smooth, unconfined horizontal ceilings where the flame height is considerably less than the ceiling height, useful correlations to quantify properties in radial direction have been developed. These correlations are widely used to calculate the response time of a fixed-temperature heat detector and/or a heat sensitive device in a sprinkler for a given fire scenario. Fewer studies [7–8] have reported on the ceiling jet flow produced by a steady fire source along an inclined smooth ceiling. Authors [9–11] also examined the effect of the ceiling inclination angle on the temperature and velocity along the steepest run in the upward direction, horizontal distribution of temperature in the spanwise direction, and the Gaussian momentum and thermal thickness of the ceiling layer with a flame height being considerably less than the ceiling height. Although flame impingement on the ceiling influences the ceiling jet, the dependence of the ceiling jet flow properties on the inclination angle has not yet been established.

The objective of this study is threefold. First, it aims to clarify the effect of the ceiling inclination angle on the temperature and velocity distributions in the ceiling layer. Second, it seeks to examine the effect of radial distance from the plume impingement point and the ceiling inclination angle on ceiling jet Gaussian momentum and thermal thickness. Third, it aims to obtain the horizontal distribution of temperature across the ceiling jet in the spanwise direction.

EXPERIMENTAL PROCEDURES

A flat, unconfined ceiling with dimensions of 2.5 m (D) × 3.0 m (L) was used as shown in Fig. 1 (ceiling dimension are the same as in Ref. [9]). This suspended ceiling was made of 12 mm thick two-ply calcium silicate boards and had a smooth surface. The inclination angle, θ, was varied between 0° and 40°. The distance along the vertical centreline of the fuel pool, from the surface of an artificial floor (2.4 m wide and 2.4 m long) to the point where the centreline intercepts the ceiling, is called the ceiling clearance, *H*. The ceiling clearance of 1.0 m was used to coincide with the experimental condition, which was done for flame not touching the ceiling, excepting the heat release rate. When the angle of sloped ceiling is 0°, 10°, and 20°, the distance of r_{down} (the distance from the point where the centreline intercepts with the ceiling to the downward edge of the suspended ceiling) was set to 0.5 m. It was set to 0.9 m for 40°. The artificial floor was set around the fuel pool, the bottom of which was adjusted to be flush with the level of the artificial floor. The fuel pool rested on an electronic balance (model LP34001S, Sartorius; accuracy: 0.1 g) for mass loss measurement.

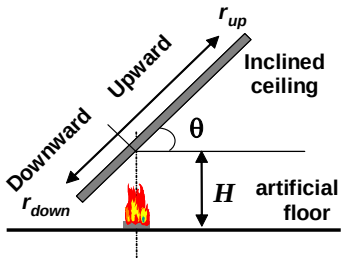

Fig. 1. Experimental arrangement.

A fuel pan with dimensions of 0.285 m × 0.285 m made from 2 mm thick stainless steel was used. The depth of a pan was 30 mm. N-heptane (Wako Pure Chemical Industries, Ltd., 99 %) was employed as the fuel. The fuel was floated on water, which is in an equal amount to the fuel, to stabilize the burning rate. The ceiling jet temperature and velocity were measured as functions of radial distance. Temperature and velocity distributions perpendicular to the sloped ceiling were also obtained. These data were measured as a function of inclination angle. Temperature and Velocity measuring positions are listed in Table 1.

Table 1. Temperature and velocity measuring positions (H = 1.0 m, D = 0.285 m).

	Measured locations, r_{up} (m)					
Angle (°)	0.4	0.8	1.2	1.6	2.0	2.4
0	X	X	X	X	X	O
10	X	X	X	X	X	O
20	X	X	X	X	X	O
40	X	X	X	X	O	

O: temperature X: temperature and velocity(PIV)

Table 2. Setting positions of bi-directional flow probe.

	Measured locations, r_{up} (m)												
Angle (°)	0.05	0.1	0.15	0.2	0.3	0.4	0.6	0.8	1.0	1.2	1.4	1.6	1.8
0	O	O		O	O	O	O	O	O	O	O	O	O
10	O		O		O	O	O	O	O	O	O	O	O
20	O		O		O	O	O	O	O	O	O	O	O
30	O		O	O	O	O	O	O	O	O	O	O	O
40	O	O	O	O	O	O	O	O	O	O	O	O	

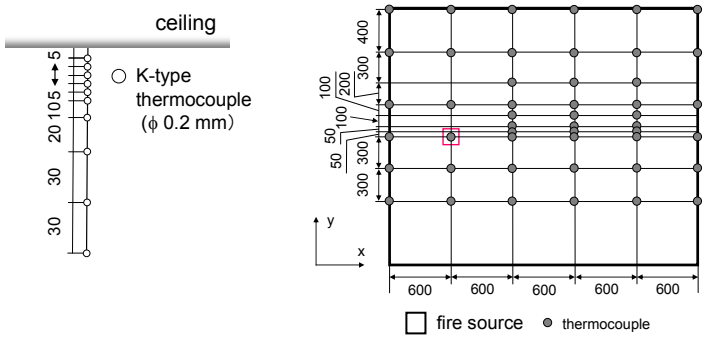

Fig. 2. Schematic diagram of thermocouple rake and positions of temperature measurement.

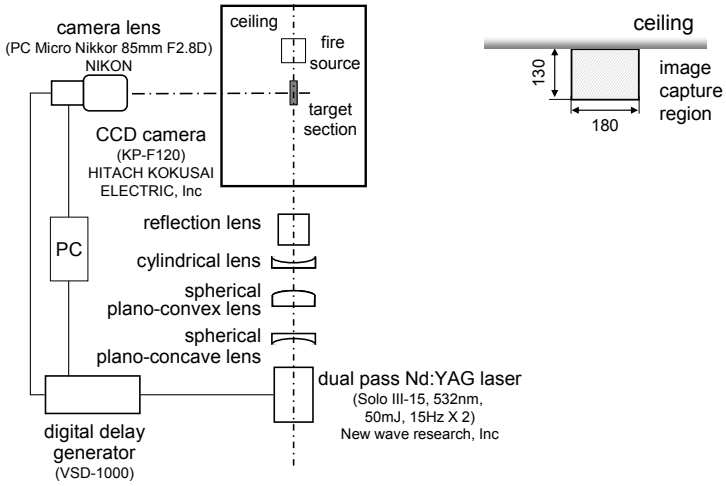

Fig. 3. Schematic diagram of PIV system.

The temperature inside the ceiling jet was measured at 10 positions (5, 10, 15, 20, 25, 30, 40, 60, 90, 120 mm from the ceiling surface) using a rake of 0.2 mm chromel-alumel thermocouples. To obtain

temperature distributions in spanwise direction of the hot current generated by a steady fire, the same type of thermocouples were installed 10 mm below the ceiling at 48 points of measurement as shown in Fig. 2. In these tests, the inclination angle of the ceiling was varied in four steps as 5°, 10°, 20° and 30° and the distance of r_{down} was set to 0.6 m.

Velocities were measured by two methods bi-directional flow probes and particle image velocimetry system (FTR-PIV, Flowtech research Inc.). The bi-directional flow probe was positioned 15 mm under the sloped ceiling and systematically measured by moving the measurement point in radial direction as shown in Table 2. The bi-directional flow probes used in this study were fabricated based on the design of McCaffrey and Heskestad [12]. Figure 3 shows the schematic diagram of PIV system employed in this study. A pair of laser sheets was pulsed every 0.067 s (15 Hz), and the total measuring duration to obtain 100 pairs velocity images was 6.7 s. Two velocity components on the two-dimensional laser sheet cross section are obtained. The measured velocity field was 180 mm × 130 mm and velocity data were obtained at 2 mm intervals. Smoke particles generated from n-heptane were used as a tracer. The velocity vectors are obtained using FtvPIV software, which calculates velocity vectors based on the cross correlation of the particle assemblage in the interrogation window by using a pair of snapshots with different time. In present experiment, the time interval to obtain a piece of velocity field image from a pair of snapshot of velocity image varied in five steps as 200, 400, 600, 800, and 1000 μs regardless of the radial distance from the plume impingement point and the ceiling inclination angle. Estimated maximum velocity and ceiling thickness, L_V, were obtained in each time interval and radial position.

Data pertaining to the temperature, velocity measured by bi-directional flow probe, and weights of the fuel were acquired in every second using a data logger (MX110, Yokogawa). Data collection began 60 s before ignition of the fuel. Each test lasted for at least 5 min. Temperature rise, velocity measured by bi-directional flow probe, and heat release rate are average values over 100 s during steady-state burning of the fuel. During each test, mechanical ventilation in the laboratory was deactivated and all the doors of the test room were closed.

DEFINITION OF PARAMETERS AND ESTIMATION METHOD OF CEILING JET THICKNESS

The ceiling jet is characterized as a function of respective maximum values, vertical distance from the ceiling, z, and radial distance from the plume impingement point, r_{up}, (i.e. $V(r_{up}, z)$ and $\Delta T\ (r_{up}, z)$). The key parameters that define the ceiling jet behaviour as a function of its position under steady-state conditions are identified in Fig. 4. The ceiling jet momentum and thermal boundary layer thickness are denoted as δV_{max} and δT_{max}, respectively. They identify a region of the ceiling jet where flow velocity and temperature vary from the wall no-slip conditions to maximum values V_{max} and ΔT_{max}. At distances beyond boundary layer thickness, the ceiling jet flow behaves like a free jet and its growth may be defined by half-Gaussian distribution. Here, momentum and thermal Gaussian thickness, L_V and L_T, are represented as a sum of boundary layer thickness and the length from the maximum point to the point where each value becomes 1/e of the maximum value, namely L_V and L_T, are represented as follows; $L_T = \delta T_{max} + L_{\Delta T_{max}/e}$, $L_V = \delta V_{max} + L_{V_{max}/e}$.

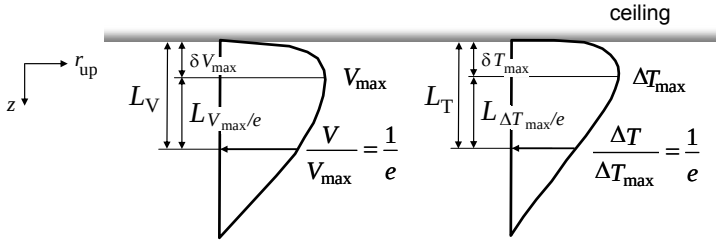

Fig. 4. Schematic of ceiling jet and its characteristic parameters.

The estimated maximum temperature and its position are based on a quadratic fit to the measured data of three points, including the measured maximum temperature and two adjoining temperatures instead of assigning the measured maximum temperature rise. The position corresponding to 1/e of the estimated

maximum temperature rise was calculated by fitting Eq. 1 to the measured data. The values of coefficients *a*, *b*, and *c* in Eq. 1 were calculated using three points: the estimated maximum temperature rise and the other two measured temperature and coordinate pairs, which placed the 1/*e* position of estimated maximum temperature between them. In the case that the application of Eq. 1 is problematic, the position of 1/*e* of the estimated maximum temperature was calculated by using the straight-line approximation to apply to adjoining four points including the 1/*e* position of estimated maximum temperature.

$$L_{\frac{\Delta T_{\max}}{e}} = a\frac{1}{\sqrt{2\pi}}\exp\left(-\frac{z^2}{2}\right) + bz + c \qquad (1)$$

Similarly to the temperature rise, the estimated maximum velocity and its position based on a quadratic fit to the measured data of three points, including measured maximum velocity and two adjoining values, were employed. As the velocity was obtained at 2 mm intervals perpendicular to the sloping ceiling, the position of 1/*e*, $L_{\mathrm{Vmax/e}}$, of the estimated maximum velocity was calculated by using the straight-line approximation to adjoining four points, which places the 1/*e* position of estimated maximum velocity among these data, instead of applying Eq. 1.

RESULTS AND DISCUSSIONS

Heat Release Rate

The heat release rate was estimated from the mass loss rate and the heat of combustion of the fuels assuming complete combustion. The heat of combustion of n-heptane was assumed to be 41.2 MJ/kg [13]. The average heat release rate is about 43.0 ± 0.3 kW.

Decrease in Maximum Velocity with Radial Distance

Our data measured using a bi-directional flow probe and differential pressure gauge (Validyne, DP103-08) under the horizontal ceiling, with flame height much smaller than the ceiling height, closely agree with Alpert's correlation [11]. It is thought that velocity obtained by bi-directional flow probe corresponds to bulk average velocity of the ceiling jet, which passes over the cross section of the bi-directional flow probe tip, from the probe shape and its low flow direction sensitivity. The probe resulted in a 5 % reduction of the signal, with the probe positioned at a 30° angle from the average flow direction [11]. However, as the velocity can be measured by the accuracy at 2 mm intervals at radially given position in the PIV measurements, the maximum value of ceiling jet can be obtained. Maximum velocity was estimated by applying a quadratic fitting to the measured data. As shown in Fig. 5a, velocities obtained by PIV are slightly higher than those measured using the bi-directional flow probe. However, there is a strong correlation between PIV and bi-directional flow probe measurements. Under the condition that the velocity obtained by PIV system assigned to estimated maximum velocity, $V_{\max}$, and that by bi-directional flow probe to bulk means velocity, V_{mean}, the variation of the ratio of $V_{\mathrm{mean}}/V_{\max}$ against V_{mean} is plotted in Fig. 5b. The value of the coefficient is extremely low in the area where velocity obtained by bi-directional flow probe becomes 0.5 m/s or less. By adopting the distance from the ceiling surface to the position where the value becomes 1/*e* of $V_{\max}$ as the characteristic length of ceiling jet and assuming the velocity distribution can be approximated as a Gaussian half distribution, the relation of $V_{\mathrm{mean}} = V_{\max}/\sqrt{2}$ is derived between V_{mean} and $V_{\max}$ at given radial positions. That is, V_{mean} is about 70 % of the maximum velocity. By applying the present experimental results into above relation, the ratio of $V_{\mathrm{mean}}/V_{\max}$ becomes 0.828 (maximum: 1.07, minimum: 0.546).

As shown in Fig. 6a, the overall properties of bulk mean velocity measured by bi-directional flow probe showed a similar dependence on radial distance regardless of the inclination angle of the ceiling. There is the feature in each region, namely continuous flame, intermittent and plume regions as would the velocity along the centreline of the fire plume in an unconfined space. The bulk mean velocity gradually becomes larger with increase of the radial distance from the impingement point in the continuous flame region, and almost shows the same dependence of velocity increase rate against radial distance regardless of the inclination angle of the ceiling. In the intermittent flame region, the bulk mean velocity remains constant

regardless of distance, the boundary value between continuous and intermittent regions moves radially away from the impingement point with increase of the inclination angle of the ceiling. In the far region where only the hot current exists, the bulk mean velocity decreases with increase of the radial distance. The slope of velocity attenuation rate curve with radial distance changes with the inclination angle

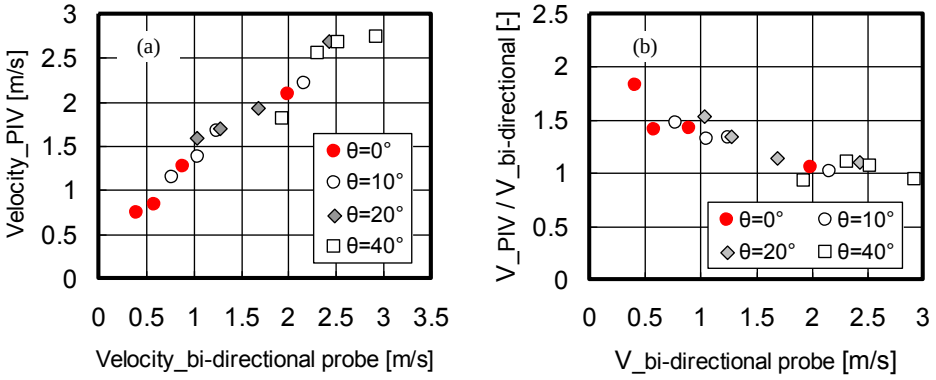

Fig. 5. Relationship between velocity obtained by PIV and by bi-directional flow probe.

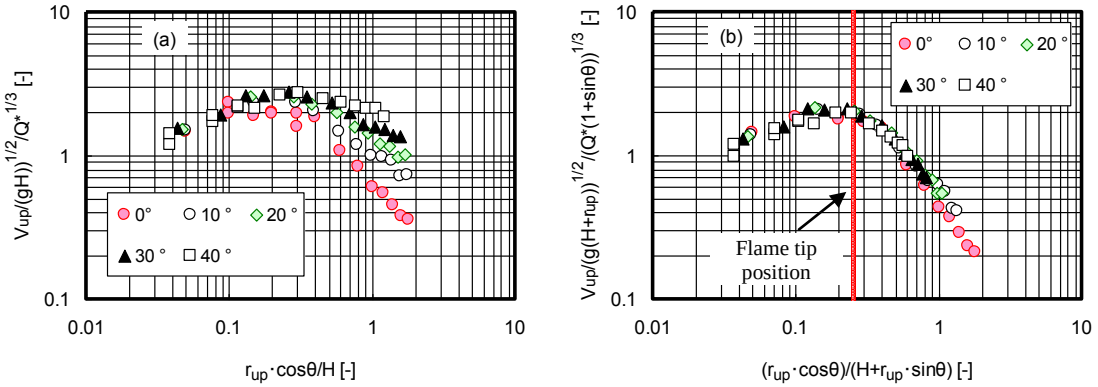

Fig. 6. Variation of velocity along steepest run in upward direction against radial distance with flame touching the inclined ceiling: (a) raw data; (b) after correction.

of the ceiling. The distance marking a change from constant velocity (intermittent zone) to decreasing velocity (thermal plume) also moves radially away from the plume axis with increase of the inclination angle. The variation of the velocity attenuation rate is due to changes in the contribution of buoyancy to the ceiling gas flow with change in angle of inclination.

In order to account for the effect of inclination angle, correction factors were introduced to heat release rate and radial distance as: (1) to express the height of the measurement point from the artificial floor surface, H was replaced with substantial height, $H + r_{up}\sin\theta$, (2) r_{up} is replaced with $H + r_{up}$, which means the origin of the ceiling jet is changed from the point where the fire plume impinges on the inclined ceiling to fire source surface and (3) dimensionless heat release rate, Q^*, is replaced with $Q^*(1 + \sin\theta)$ based on the following argument. The hot current spreads in concentric circles with the impingement point at the centre and the same quantity of hot current flows out in all directions under the horizontal ceiling. However, the mass flow rate of hot current changes depending on the hot current flow direction under the sloped ceiling. It is thought that the mass flow rate of hot current in the upward direction along the ceiling becomes large. To incorporate this influence, the contribution of heat release rate to the hot current flow was therefore changed to reflect the inclination angle of the ceiling.

By adopting these new parameters, the effect of the inclination angle of the ceiling can be accounted for and the dispersion in results between data for all angles became small as shown in Fig. 6b. The values of

coefficients α, β were decided by applying the power function to data in each region in Fig. 6b and by matching two values at the boundary value, which were obtained from each straight line.

$$\frac{V_{up}}{\sqrt{g(H+r_{up})}} \Big/ \{Q^*(1+\sin\theta)\}^{1/3} = \alpha \left(\frac{r_{up}\cdot\cos\theta}{H+r_{up}\cdot\sin\theta} \right)^{\beta} \qquad (2)$$

for $0.4 \le r/H \le 2.0$, $0° \le \theta \le 40°$

$r_{up}\cos\theta/(H+r_{up}\sin\theta) \le 0.128$ $\quad \alpha = 5.15, \quad \beta = 0.459$

$0.128 < r_{up}\cos\theta/(H+r_{up}\sin\theta) \le 0.296$ $\quad \alpha = 2.00, \quad \beta = 0$

$0.296 < r_{up}\cos\theta/(H+r_{up}\sin\theta)$ $\quad \alpha = 0.595, \quad \beta = -0.998$

Decrease in Maximum Temperature Rise with Radial Distance

The estimated maximum temperature and its position based on a quadratic fit to the measured data were employed as mentioned above. These values were calculated from the temperature distribution obtained from the thermocouple rakes installed at each location. It was first confirmed that the temperature rise under the flat, unconfined and horizontal ceiling, with flame height much smaller than the ceiling height, closely agreed with Heskestad and Delichatsios' correlation [11]. As with velocity, the temperature rise also increased with the increase of the inclination angle as shown in Fig. 7a.

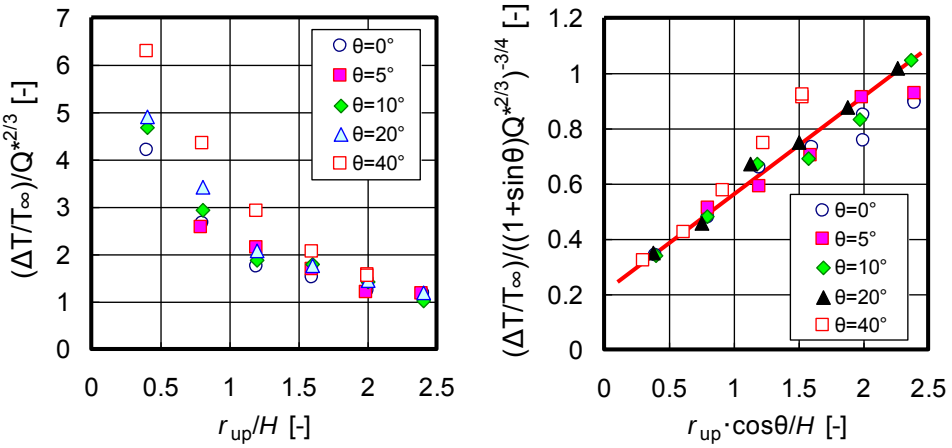

(a) (b)

Fig. 7. Variation of temperature rise along the steepest run in upward direction against radial distance with flame touching the inclined ceiling: (a) raw data; (b) after correction.

Entrainment of ambient air is a major mechanism responsible for decreasing the ceiling gas temperature. The influence of heat release rate contributed to the ceiling jet under the sloped ceiling is different from that under the horizontal ceiling. It is also thought that the mass flow rate of hot current in the upward direction along the ceiling becomes large as mentioned above. To take into account this effect of the inclination angle of the ceiling, the correction factors were introduced in terms of heat release rate and radial distance as; (1) dimensionless heat release rate, Q^*, is replaced with $Q^*(1 + \sin\theta)$ as well as velocity arrangement (2) the radial distance along the sloped ceiling is replaced to the projected distance. Coefficients in Eq. 3 are decided by applying the liner square approximation as shown in Fig. 7b.

$$\left(\frac{\Delta T}{T_\infty}\right) \Big/ \{Q^*(1+\sin\theta)\}^{2/3} = \left(0.210 + 0.352\frac{r_{up}\cos\theta}{H}\right)^{-4/3} \qquad 0.1 \le r_{up}\cos\theta/H \le 2.5 \qquad (3)$$

Ceiling Jet Gaussian Momentum and Thermal Thickness

As shown in Figs. 6a and 7a and Fig. 8, both maximum values of velocity and temperature rise gradually increase with increase of the inclination angle of the ceiling. Both vertical distribution of velocity and temperature rise at 0°, 20° and 40° changes their shape from steep distribution to gentle distribution with the increase in distance from the impingement point, r_{up} shown in Fig. 8. In the case of θ = 40°, the

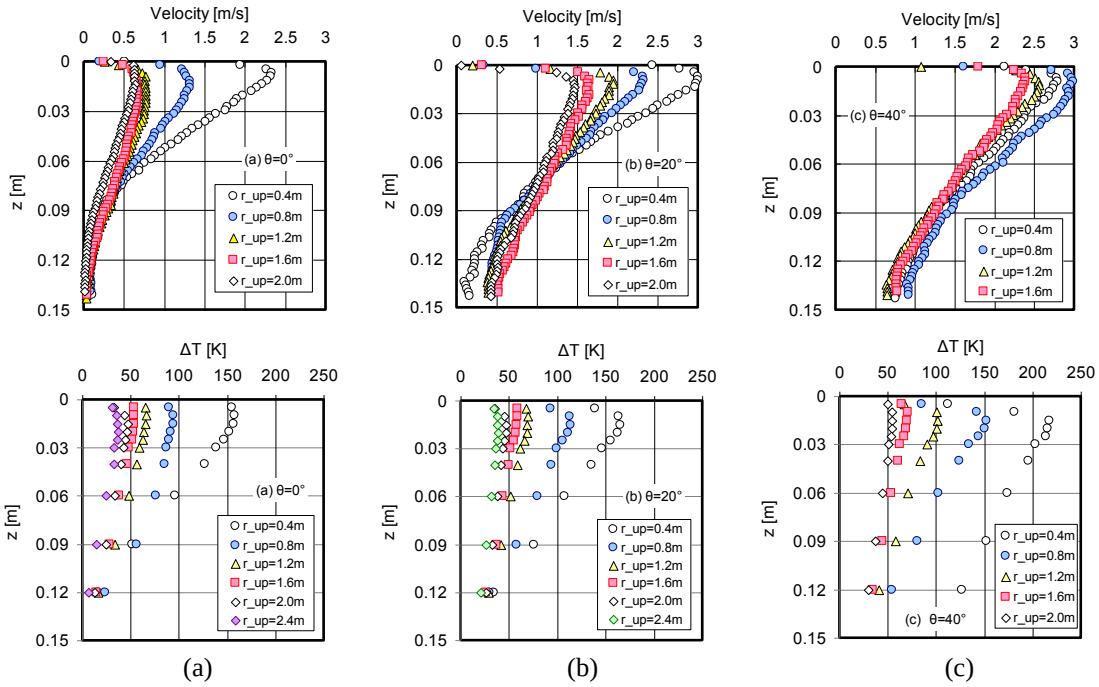

Fig. 8. Typical velocity and temperature rise distributions: (a) θ = 0°; (b) θ = 20°; (c) θ = 40°.

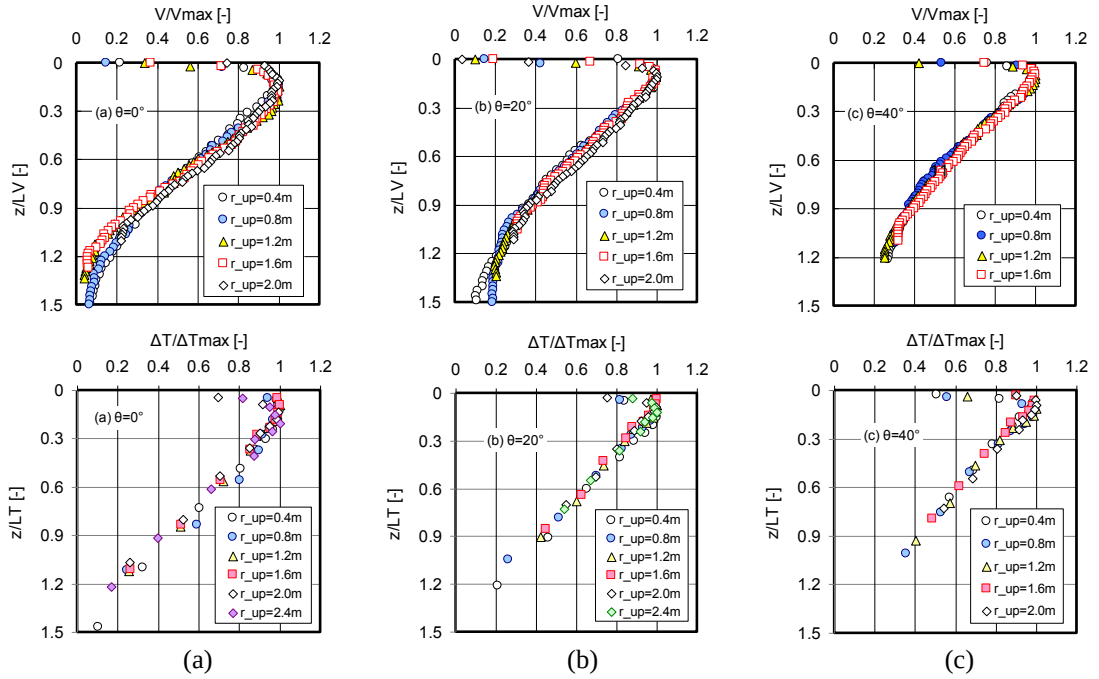

Fig. 9. Normalized velocity and temperature rise distributions: (a) θ = 0°; (b) θ = 20°; (c) θ = 40°.

maximum velocity at r_{up} = 0.4 m is smaller than that of r_{up} = 0.8 m because the velocity at r_{up} = 0.4 m corresponds to the velocity in the continuous flaming region. To examine the generality of these distributions and their shape, the method which Motevalli et al. [4] was applied to our measured data under the horizontal ceiling. Velocity and temperature rise distributions shown in Fig. 9 are normalised by dividing the perpendicular distance to the sloped ceiling with Gaussian momentum and thermal thickness, L_V and L_T, and measured values of velocity and temperature by the estimated maximum values, V_{max} and ΔT_{max}, for each measurement point. The position of $L_{Vmax/e}$ was calculated using mentioned above method, and the position of $L_{\Delta T_{max}/e}$ was also obtained by applying Eq. 1 to the measured data as shown in Fig. 10.

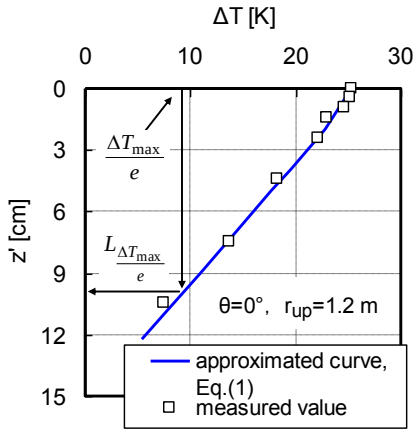

Fig. 10. A typical result for representing how to estimate the position of $L_{\Delta T_{max}/e}$.

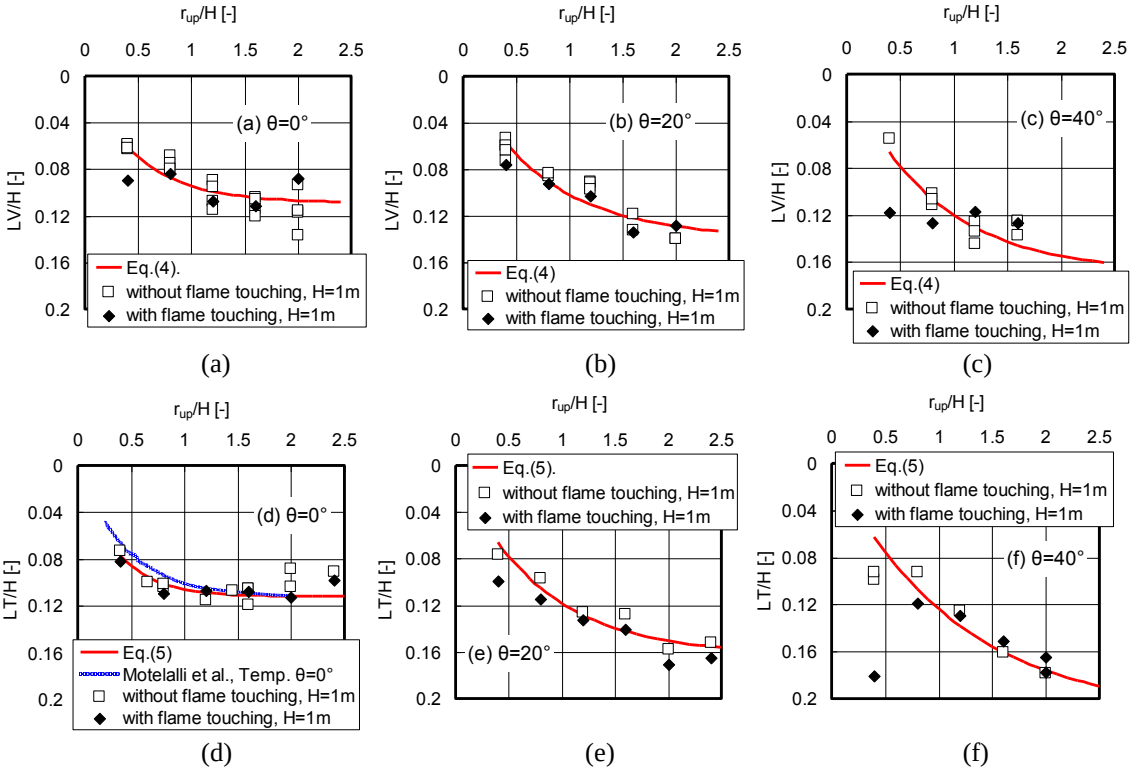

Fig.11. Dependence of L_V/H and L_T/H on ceiling inclination angle and the radial distance from the plume impingement point. Gaussian momentum thickness: (a) θ = 0°; (b) θ = 20°; (c) θ = 40°; Gaussian thermal thickness, (d) θ = 0°; (e) θ = 20°; (f) θ = 40°.

As shown in Fig. 9, it becomes clear that vertical velocity and temperature rise distributions can be represent by normalized distance, temperature rise and velocity regardless of the inclination angle of the ceiling.

To obtain vertical distribution of the ceiling jet, it is necessary to estimate the normalized distance from the ceiling and to make clear the dependence of the Gaussian momentum and temperature thickness on radial distance and inclination angle. To check this dependence, the estimated Gaussian momentum and temperature thickness in the case of flame touching the inclined ceiling were plotted with the data obtained for the case of flame not touching the inclined ceiling [11] as shown in Fig. 11. The open square symbol denotes the data in flame not touching the ceiling, and closed diamonds denotes data where the flame touches the ceiling. The solid lines in these figures were obtained based on the empirical formula for Gaussian momentum and temperature thickness in the case of flame not touching the inclined ceiling and was represented as follows:

$$\frac{L_V}{H} = \alpha_{V2}\left[1-\exp\left(\beta_{V2}\frac{r_{up}}{H}\right)\right] \qquad \alpha_{V2} = 1.47\mathrm{E}-03\cdot\theta+1.10\mathrm{E}-01 \tag{4}$$

$$\beta_{V2} = -1.86+0.672\left[1-\exp\left(-0.0953\cdot\theta\right)\right]$$

$$\text{for } 0.4\le(r_{up}/H)\le 2.0,\quad 0^{o}\le\theta\le 40^{o}$$

$$\frac{L_T}{H} = \alpha_{T2}\left[1-\exp\left(\beta_{T2}\frac{r_{up}}{H}\right)\right] \qquad \alpha_{T2} = 2.54\mathrm{E}-03\cdot\theta+1.12\mathrm{E}-01 \tag{5}$$

$$\beta_{T2} = -2.91+2.20\left[1-\exp\left(-0.0662\cdot\theta\right)\right]$$

$$\text{for } 0.4\le(r_{up}/H)\le 2.4,\quad 0^{o}\le\theta\le 40^{o}$$

To confirm the applicability of Eqs. 4 and 5, the relative error between the measured data and Eq. 6 is shown in Table 3. It can be confirmed that the thickness of the ceiling jet in the case of flame touching the inclined ceiling almost corresponds to the thickness in the case of flame not touching from these series of results, if the data in continuous flame region is excluded.

Table 3. Relative error.

θ (°)	ε		Note
	Temperature	**Velocity**	
0	0.0260	0.0783	
10	0.0405	0.0272	
20	0.0536	0.0459	
40	0.1380	0.1308	
	0.0289	0.0815	data of r = 0.4 m is excluded

$$\varepsilon = \frac{\sum\sqrt{\frac{(x_i-y_i)^2}{n}}}{\sum\sqrt{y_i^{\,2}}} \tag{6}$$

where x_i : measured data
y_i : calculated data by Eqs. 4 or 5
n : number of data

TEMPERATURE DISTRIBUTION IN SPANWISE DIRECTION

A similar technique as represented in Eq. 7 was applied to estimate the dependence of temperature spread width in spanwise direction of the ceiling jet in flame touching the ceiling on the inclination angle.

$$\frac{\Delta T_{\text{spanwise}L}}{\Delta T_{up,L}} = \exp\left(-\gamma^2 \cdot \eta^2\right),\ \eta = r_{span}/L,\ L = H/\sin\theta + r_{up},\ \gamma = 15.6\,\theta^{-0.55} \quad (7)$$

It is clear from the isothermal curves constructed using the measured temperatures that the hot current flows radially in all directions just after impinged on the sloped ceiling and changes its flow direction along the inclined ceiling. Finally, the isothermal curves show the shape that expands like the oval along the sloped ceiling. In order to examine the temperature distribution in the spanwise direction for the case of flame touching the inclined ceiling, normalised temperatures denoted by $\Delta T_{\text{spanwise,L}}/\Delta T_{\text{up,L}}$ at each point were plotted against dimensionless distance, η, as shown in Fig. 12. Although there is significant scatter in the data for each angle of the ceiling, a straight line approximated by least squares method was obtained for each condition, and the values of γ determined from the gradient of the straight line. It is confirmed that the dependence of the spread width on the inclination angle of the ceiling for cases where the flame touched the ceiling almost coincided with that for cases when the flame did not touch the ceiling as shown in Fig. 13. According to Eq. 6, the relative error was calculated and becomes 0.0770.

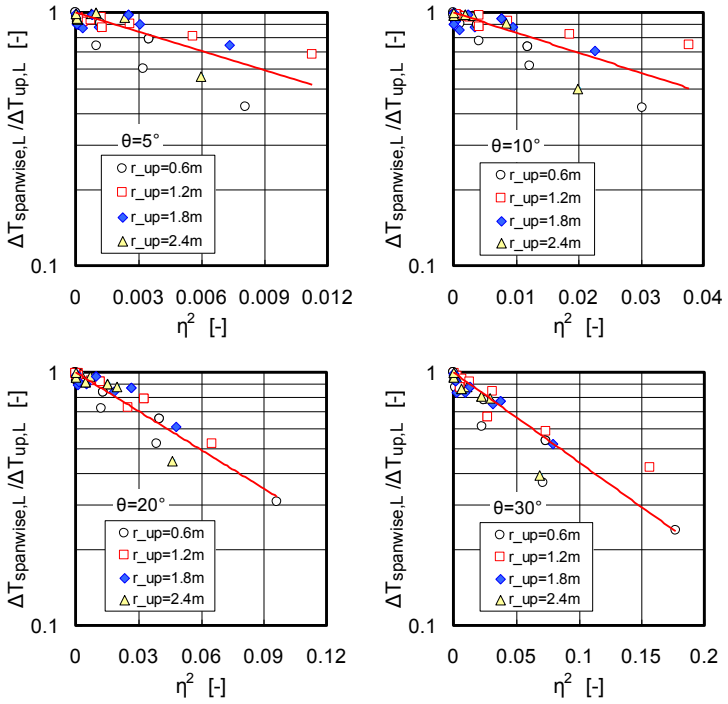

Fig. 12. Spread width of temperature distribution at each inclined ceiling.

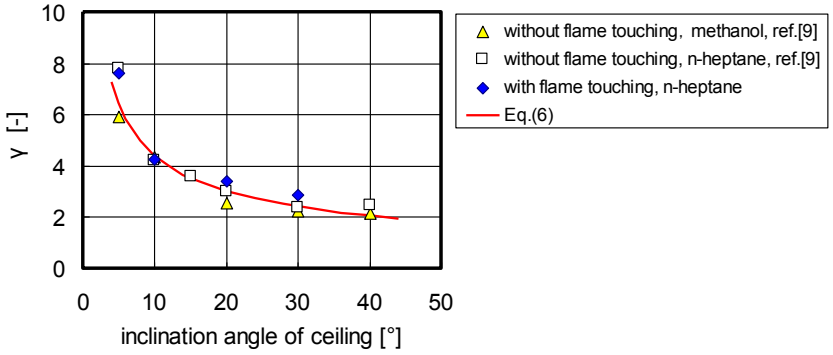

Fig. 13. Dependence of spread width against the inclination angle of the ceiling.

CONCLUSIONS

Based on a series of ceiling jet experiments with flames impinging on a sloped ceiling, the following conclusions are reached:

1) An empirical correlation between decrease in maximum temperature rise and radial distance along a sloped ceiling was found by modifying the terms of radial distance and heat release rate used in correlations for small fires under horizontal ceilings.
2) An empirical formula for the relationship between velocity decrease and radial distance in the upward direction was developed by introducing new correction factors for height, distance, and heat release rate.
3) Vertical temperature rise and velocity distributions can be represented in terms of normalized distance, temperature rise, and velocity regardless of the inclination angle of the ceiling.
4) Gaussian momentum and thermal thickness of the ceiling jet for flames touching the inclined ceiling are very similar to those for flames not touching the inclined ceiling.
5) Dependence of spread width of temperature in the spanwise direction against the inclination angle of the ceiling in flame touching the inclined ceiling is very similar to that for cases in which the flame is not touching the inclined ceiling.

REFERENCES

[1] Alpert, R.L., "Fire Induced Turbulent Ceiling Jet", Technical Report, Factory Mutual Research Corp., FMRC Serial No. 19722-2, 1971.

[2] Alpert, R.L., (1975) Turbulent Ceiling Jet Induced by Large-Scale Fires, Combustion Science and Technology, 11: 197-213. http://dx.doi.org/10.1080/00102207508946699

[3] Heskestad, G. and Delichatsios, M.A., "The Initial Convective Flow in Fire", *Proc. of 17th International Symposium on Combustion*, pp.1113, The Combustion Inst., 1978.

[4] Motevalli, V. and Marks, C.H., 1991. Characterizing The Unconfined Ceiling Jet Under Steady-state Conditions: A Reassessment. *Fire Safety Science* 3: 301-312. http://dx.doi.org/10.3801/IAFSS.FSS.3-301

[5] Cooper, L.Y., "Ceiling Jet-Driven Wall Flows in Compartment Fires", NBSIR 87-3535, National Bureau of Standards, Gaithersburg, MD, USA, 1987.

[6] You, H.Z. and Feath, G.M., "Investigation of Fire Impingement on a Horizontal Ceiling", NBS-GCR-79-188, National Bureau of Standards, Gaithersburg, MD, USA, 1978.

[7] Kung, H.C., Spaulding, R.D. and Stavrianidis, P., 1991. Fire Induced Flow under A Sloped Ceiling. *Fire Safety Science* 3: 271-280. http://dx.doi.org/10.3801/IAFSS.FSS.3-271

[8] Sugawa, O., (2001) Simple Estimation Model on Ceiling Temperature and Velocity of Fire Induced Flow under Ceiling, Fire Science and Technology, 12(1): 57-67.

[9] Oka, Y., Imazeki, O. and Sugawa, O., (2010) Temperature Profile of Ceiling Jet Flow along an Inclined Unconfined Ceiling, Fire Safety Journal, 45: 221-227. http://dx.doi.org/10.1016/j.firesaf.2010.03.003

[10] Oka, Y. and Ando, M., "Temperature and Velocity Decreasing Property of Ceiling Jet Impinged on an Unconfined Inclined Ceiling", submitted to Fire Safety Journal.

[11] Oka, Y. and Imazeki, O., "Influence of Inclination Angle of Ceiling on Ceiling Jet Property", *Proceedings of the 8th Asia-Oceania Symposium on Fire Science and Technology*, Melbourne, Australia, 2010.

[12] McCaffrey, B.J. and Heskestad, G., (1976) A Robust Bidirectional Low Velocity Probe for Flame and Fire Application, Combustion and Flame, 26: 125-127. http://dx.doi.org/10.1016/0010-2180(76)90062-6

[13] Tewarson, A., "Generation of Heat and Chemical Compounds in Fires", *The SFPE Handbook of Fire Protection Engineering (3rd ed.)*, Section 3, Chapter 4, 2002.